ELSEVIER

Surface Science 473 (2001) 50–58

SURFACE SCIENCE

www.elsevier.nl/locate/susc

Angular distribution of electrons elastically backscattered from amorphous overlayer systems

C.M. Kwei [a,*], S.S. Tsai [a], C.J. Tung [b]

[a] *Department of Electronics Engineering, National Chiao Tung University, Hsinchu 300, Taiwan, ROC*
[b] *Department of Nuclear Science, National Tsing Hua University, Hsinchu 300, Taiwan, ROC*

Received 1 September 2000; accepted for publication 30 October 2000

Abstract

Monte Carlo calculations have been performed of the angular distribution of electrons elastically backscattered from amorphous overlayer systems composed of thin copper films and semi-infinite silicon substrates. These calculations showed that the angular distribution of the elastically reflected intensity was dependent on film thickness and electron energy. They also showed that elastically backscattered electrons were due substantially to one, two and three scatterings with single-scattering events contributing about half of the intensity. Based on these findings, we have derived a formula for the contribution from single-scattering events to the angular distribution of the elastically reflected intensity. Combining this formula and the P_1-approximation for multiple scattering, we were able to construct an analytic formula for the angular distribution of electrons elastically backscattered from overlayer systems. Results from this approach were in good agreement with those computed using Monte Carlo simulations.

Keywords: Electron–solid interactions, scattering, diffraction; Monte Carlo simulations; Semi-empirical models and model calculations; Copper; Silicon; Metal–semiconductor interfaces

1. Introduction

Analysis of the elastic peak in the spectrum of electrons backscattered from solid surfaces is important in surface sensitive electron spectroscopies [1,2]. This analysis in elastic peak electron spectroscopy [3–8], for instance, has attracted much attention because of its application to the experimental determination of electron inelastic mean free paths in solid targets. The features of elastic peak spectra are characterized by the angular distribution of the intensity for elastically backscattered electrons.

Several theoretical approaches are available for the evaluation of elastic peak electron spectra. Schilling and Webb [9] proposed a fitting model using the sharp forward scattering approximation for twice-scattered electrons and a uniform background approximation for multiply scattered electrons. These approximations seem not plausible for accurate evaluation of elastically backscattered electrons. Tofterup [10] employed a

* Corresponding author. Tel.: +886-3-5712121, ext.: 54136; fax: +886-3-5727300.
E-mail address: cmkwei@cc.nctu.edu.tw (C.M. Kwei).

0039-6028/01/$ - see front matter
PII: S0039-6028(00)00953-5

P_1-approximation by solving the Boltzmann transport equation in terms of two Legendre polynomials for the angular distribution of elastically backscattered electrons. This treatment seems good for multiple scatterings, i.e. many small angle scatterings, but inadequate for single and plural, or very few, elastic scatterings. Chen et al. [11] later applied the Monte Carlo (MC) method to analyze the elastic reflection intensity of electrons elastically backscattered from semi-infinite systems. The MC results indicated that the elastically backscattered intensity was substantially due to only a few scatterings with single-scattering events contributing approximately half of the intensity. Therefore, they suggested the approach of evaluating the contribution from one, two and three scatterings exactly and higher order scatterings by the P_1-approximation. Calculated results were in good agreement with those using MC simulations and with experimental data.

In the present paper, the angular distribution of electrons elastically backscattered from overlayer systems was studied. Previously, Jablonski et al. [12] made use of step-function-like electron inelastic mean free paths for volume excitations of the constituent materials in their MC simulations to study this distribution. Recently, Kwei et al. [13] constructed depth-dependent electron inelastic mean free paths by considering all relevant interactions including volume excitations, surface (vacuum–film interface) excitations and interface (film–substrate interface) excitations. In this work, we applied these spatial-varying electron inelastic mean free paths in MC simulations for the angular distribution of electrons elastically backscattered from vacuum-Cu–Si overlayer systems. It was found that approximately half of the elastically backscattered electrons had been scattered once. Therefore, we have derived a formula for the contribution from single-scattering events to the angular distribution of the elastically reflected intensity. Combining this formula and the P_1-approximation for multiple scatterings, we were able to construct analytically the angular distribution of electrons elastically backscattered from overlayer systems. Results calculated based on such formulas were in good agreement with those computed using MC simulations.

2. Monte Carlo simulations

The MC method has been widely applied in the study of electron reflection phenomena [4,7]. Previously, we have simulated electrons backscattered from semi-infinite solids [14–16]. Here we apply this method to compute the angular distribution of electrons elastically backscattered from overlayer systems. In the MC method, uniformly distributed random numbers between 0 and 1 are generated to determine electron elastic scatterings, scattering angles and step lengths according to the differential and total elastic cross-sections. The trajectories of elastically backscattered electrons in the overlayer systems are traced by recording electron coordinates as well as polar and azimuthal scattering angles.

For overlayer systems consisting of two media, i.e. film A and substrate B, the polar scattering angle θ relative to the propagation directions before and after each elastic scattering is determined by the random number R_1 as

$$R_1 = \begin{cases} N_A \lambda_e^A \int_0^\theta \left(\frac{d\sigma}{d\Omega}\right)_A 2\pi \sin\theta \, d\theta, \\ \quad \text{if the electron is within the film,} \\ N_B \lambda_e^B \int_0^\theta \left(\frac{d\sigma}{d\Omega}\right)_B 2\pi \sin\theta \, d\theta, \\ \quad \text{if the electron is within the substrate.} \end{cases} \tag{1}$$

Here N_A and N_B are the number of atoms per unit volume in media A and B, respectively, $(d\sigma/d\Omega)_A$ and $(d\sigma/d\Omega)_B$ are the corresponding elastic differential cross-sections, and λ_e^A and λ_e^B are the corresponding electron elastic mean free paths given by

$$(\lambda_e^A)^{-1} = N_A \int \left(\frac{d\sigma}{d\Omega}\right)_A d\Omega \tag{2}$$

and

$$(\lambda_e^B)^{-1} = N_B \int \left(\frac{d\sigma}{d\Omega}\right)_B d\Omega. \tag{3}$$

In this work, elastic differential cross-sections are calculated using the partial wave expansion method with the finite difference technique for solids using the Hartree–Fock–Wigner–Seitz potential. The azimuthal scattering angle is determined by

$$\phi = 2\pi R_2 \tag{4}$$

through the random number R_2. Applying Poisson statistics, the step length S for electrons traveling between two successive interactions in one of the solids, either A or B, is determined through another random number by the relation

$$S = -\lambda_e \ln R, \tag{5}$$

where λ_e is the electron elastic mean free path in that solid. For overlayer systems, the $(j+1)$th elastic scattering at position z_{j+1} following the jth elastic scattering at position z_j with scattering angle Θ_j relative to the surface normal is determined by the random number R_3 through

$$\frac{1}{\cos\Theta_j}\int_{z_j}^{z_{j+1}} \frac{dz}{\lambda_e(z)} = -\ln R_3, \tag{6}$$

where the position-dependent elastic mean free path is given by

$$\lambda_e(z) = \begin{cases} \lambda_e^A, & \text{if } z \text{ is within the film,} \\ \lambda_e^B, & \text{if } z \text{ is within the substrate.} \end{cases} \tag{7}$$

Here Θ_j may be related to the polar and azimuthal scattering angles θ_j and ϕ_j through

$$\cos\Theta_j = \cos\Theta_{j-1}\cos\theta_j - \sin\Theta_{j-1}\sin\theta_j\cos\phi_j, \tag{8}$$

where Θ_{j-1} is the scattering angle relative to the surface normal for an electron before the jth elastic scattering.

The tracking of electrons continues until either they are backscattered from the solid or their trajectory lengths in the solid become so large that any attainable contribution to the backscattered electron intensity can be neglected. The elastic reflection intensity is then given by

$$I = \frac{1}{n}\sum_{i=1}^{n}\Delta I_i, \tag{9}$$

where ΔI_i is the intensity of elastically backscattered electrons into acceptance angles for the ith trajectory and n is the total number of sampled trajectories. The probability that an electron travels from z_j to z_{j+1} along the direction Θ_j without any energy loss is given by

$$P_0 = \exp\left(-\frac{1}{\cos\Theta_j}\int_{z_j}^{z_{j+1}}\frac{1}{\lambda_i(z)}dz\right), \tag{10}$$

where $\lambda_i(z)$ is the depth-dependent electron inelastic mean free path. In this work, the electron inelastic mean free path is calculated using dielectric response theory in which volume, surface (vacuum–film interface) and interface (film–substrate interface) excitations are considered [13]. Note that the inelastic mean free path is different for injected and ejected electrons [13]. When z_{j+1} is closer to the surface than z_j, for instance, we use the inelastic mean free path for ejected electrons. Note also that surface excitations are possible for electrons traveling outside the solid. The probability that an electron from the vacuum crosses the surface at angle α relative to the surface normal without exciting the surface is $\exp[-P_s(\alpha)]$ [14], where the surface excitation parameter is given by [17]

$$P_s(\alpha) = \frac{1}{\cos\alpha}\int_{-\infty}^{0}\frac{1}{\lambda_i(z)}dz \tag{11}$$

with $\lambda_i(z)$ appropriate for either injected or ejected electrons. The integration in Eq. (11) is carried out over electron distance from the surface outside the solid. Thus, ΔI_i may be obtained by tracing the linear step lengths between elastic scattering events.

3. Theory

Consider an overlayer system composed of a film A of thickness d on a substrate B. The probability function for the normally incident electron reaching a depth z before any elastic scattering is given by Poisson statistics as

$$F_1(z) = \begin{cases} \frac{1}{\lambda_e^A}\exp\left(-\frac{z}{\lambda_e^A}\right), & \text{when } z < d, \\ \frac{1}{\lambda_e^B}\exp\left(-\frac{d}{\lambda_e^A}\right)\exp\left(-\frac{z-d}{\lambda_e^B}\right), & \text{when } z > d, \end{cases} \tag{12}$$

where λ_e^A and λ_e^B are electron elastic mean free paths in the film and the substrate, respectively. At depth z, an elastic scattering occurs. The probability function of electrons elastically backscat-

tered into the differential solid angle $d\Omega_1$ around (θ_1, ϕ_1) is given by

$$P_\Omega(\theta_1,\phi_1)\,d\Omega_1 = \begin{cases} \frac{1}{\sigma_e^A}\left(\frac{d\sigma}{d\Omega}\right)_A^{\theta_1} d\Omega_1, & \text{when } z < d, \\ \frac{1}{\sigma_e^B}\left(\frac{d\sigma}{d\Omega}\right)_B^{\theta_1} d\Omega_1, & \text{when } z > d, \end{cases} \tag{13}$$

where θ_1 is the polar scattering angle, ϕ_1 is the azimuthal scattering angle, $d\Omega_1 = \sin\theta_1 d\theta_1 d\phi_1$ is the differential solid angle, $(d\sigma/d\Omega)_A^{\theta_1}$ and $(d\sigma/d\Omega)_B^{\theta_1}$ are electron elastic differential cross-sections in film A and substrate B for polar scattering angle θ_1, and σ_e^A and σ_e^B are the total electron elastic-scattering cross-sections in media A and B. After the scattering, the probability function for the exit electron reaching the surface without further elastic scattering is given by

$$F_R(z) = \begin{cases} \exp\left(-\frac{z}{\lambda_e^A \cos\alpha}\right), & \text{when } z < d, \\ \exp\left(-\frac{d}{\lambda_e^A \cos\alpha}\right)\exp\left(-\frac{z-d}{\lambda_e^B \cos\alpha}\right), & \text{when } z > d, \end{cases} \tag{14}$$

where α is the escape angle relative to the surface normal.

The probability that a normally incident electron penetrates to depth z without any inelastic interaction is given by

$$G_I(z) = \exp\left(-\int_0^z \frac{dz'}{\lambda_i^I(z')}\right), \tag{15}$$

where $\lambda_i^I(z')$ is the injected electron inelastic mean free path at depth z'. After an elastic scattering at depth z, the probability that the electron leaves the surface with an escape angle α without any inelastic interaction is given by

$$G_R(z) = \exp\left(-\int_0^z \frac{dz'}{\lambda_i^R(z')\cos\alpha}\right), \tag{16}$$

where $\lambda_i^R(z')$ is the ejected electron inelastic mean free path at depth z'. Therefore, the angular distribution contributed from a single-elastic scattering to the elastic reflection intensity of electrons backscattered with escape angle α is then given by

$$H_1(\alpha) = \frac{1}{2\pi\sin\alpha} e^{-P_s(0)} e^{-P_s(\alpha)} P_\Omega(\pi-\alpha,\phi_1) \times \int_0^\infty F_I(z)F_R(z)G_I(z)G_R(z)\,dz, \tag{17}$$

where the surface excitation parameter, $P_s(0)$ and $P_s(\alpha)$, is calculated using Eq. (11) for injected and ejected electrons. The exponential factors in Eq. (17) represent the probability that an electron in vacuum crosses the surface without surface excitations. The elastically reflected intensity contributed by a single-elastic scattering for backscattered electrons with escape angle between α_1 and α_2 may be obtained by

$$\eta_1(\alpha_1,\alpha_2) = \int_{\alpha_1}^{\alpha_2} H_1(\alpha)\,d\Omega_1. \tag{18}$$

Let $H_i(\alpha)$ be the angular distribution contributed from i scatterings to the elastic reflection intensity of electrons backscattered with escape angle α and η_i be the corresponding elastic reflection intensity for backscattered electrons with escape angle between 0 and $\pi/2$, i.e. $\eta_i = \eta_i(0,\pi/2)$. The normalized distribution of elastically backscattered electrons can be calculated using

$$I(\alpha) = \sum_{i=1}^{\infty} \frac{\eta_i}{\eta} I_i(\alpha), \tag{19}$$

where $\eta = \Sigma_{i=1}^{\infty}\eta_i$ is the total elastically reflected intensity and $I_i(\alpha) = H_i(\alpha)/\eta_i$ is the normalized angular distribution of elastically backscattered electrons contributed by i scatterings. Using the P_1-approximation, the normalized angular distribution is given by [10]

$$I^{P_1}(\alpha) = \frac{1}{2\pi}\left(\frac{3}{2}\cos^2\alpha + \cos\alpha\right). \tag{20}$$

In this work, we use Eqs. (17) and (18) for $I_1(\alpha)$ and the P_1-approximation for $I_i(\alpha)$ with $i \geqslant 3$. For $i = 2$, a fitting model with appropriate combination of the single-scattering model and the P_1-approximation is proposed. We take

$$I_2(\alpha) = aI_1(\alpha) + (1-a)I^{P_1}(\alpha), \tag{21}$$

where a is the fitting parameter. The normalized total angular distribution is then given by

$$I(\alpha) = \left(\frac{\eta_1}{\eta} + \frac{a\eta_2}{\eta}\right) I_1(\alpha) + \left[\frac{(1-a)\eta_2}{\eta} + \sum_{i \geqslant 3} \frac{\eta_i}{\eta}\right] \times I^{P_1}(\alpha). \quad (22)$$

4. Results and discussion

The MC algorithm described above was applied to simulate electrons elastically backscattered from vacuum-Cu–Si overlayer systems of different Cu film thicknesses. The basic inputs in the MC simulations were the differential elastic cross-sections and the depth-dependent inelastic mean free paths of the electrons. Fig. 1 shows differential elastic cross-sections calculated using the partial wave expansion method and the finite difference technique for 300, 500 and 800 eV electrons in Cu. A similar plot in Si is shown in Fig. 2. In both cases, the elastic scattering potentials were derived from the Hartree–Fock–Wigner–Seitz electron density distribution of solid atoms. The use of electron density distribution of solid atoms instead of free atoms reduces differential elastic cross-sections at small scattering angles. A comparison between Figs. 1 and 2 indicates that the differential elastic cross-sections at large scattering angles, corresponding to the contribution from single-scattering events to the backscattered intensity, are larger for Cu than for Si. At small scattering angles, where multiple-scattering events are important, the differential elastic cross-sections in Cu are somewhat smaller than in Si.

Fig. 3 shows inelastic inverse mean free paths for 300 eV electrons normally escaping from a vacuum-Cu–Si overlayer system for different Cu film thicknesses as a function of electron depth in the system. These depth-dependent electron inelastic mean free paths were calculated using an extended Drude-type dielectric function derived from experimental optical data [18]. A detailed description of the model calculations was given previously [13]. It is seen in Fig. 3 that the electron inelastic inverse mean free path extends to a few angstroms outside the solid (negative z) due to surface excitations. Inside the solid (positive z), variations in electron inelastic inverse mean free path near the surface and interface were found due to surface (vacuum–film interface) and interface (film–substrate interface) excitations. As the thickness of the Cu film decreases, the electron inelastic inverse mean free path in the overlayer

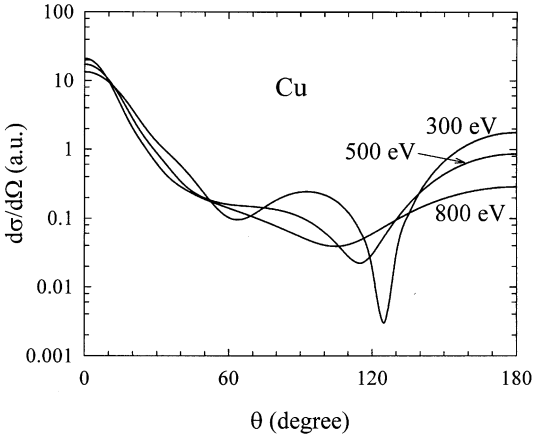

Fig. 1. A plot of the elastic differential cross-section, in atomic units, as a function of scattering angle for electrons of several energies in Cu. Results were calculated using the partial wave expansion method and the finite difference technique for a Hartree–Fock–Wigner–Seitz scattering potential of solid Cu.

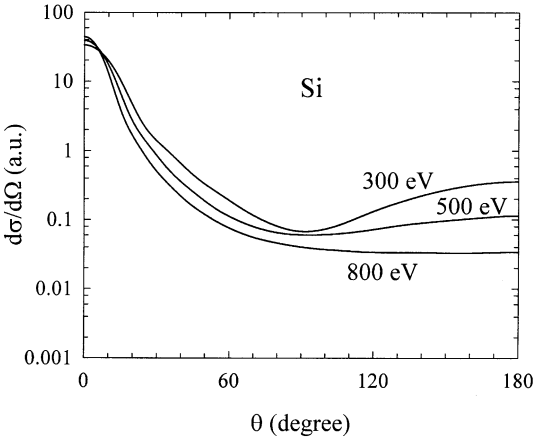

Fig. 2. A plot of the elastic differential cross-section, in atomic units, as a function of scattering angle for electrons of several energies in Si. Results were calculated using the partial wave expansion method and the finite difference technique for a Hartree–Fock–Wigner–Seitz scattering potential of solid Si.

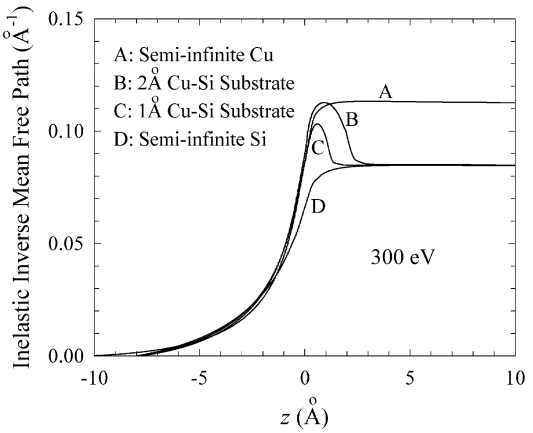

Fig. 3. The depth-dependent inelastic inverse mean free path for a 300 eV electron normally escaping from a vacuum-Cu–Si overlayer system with different Cu film thicknesses as a function of electron depth in the system. Results were calculated using an extended Drude-type dielectric function [13] derived from experimental optical data [18].

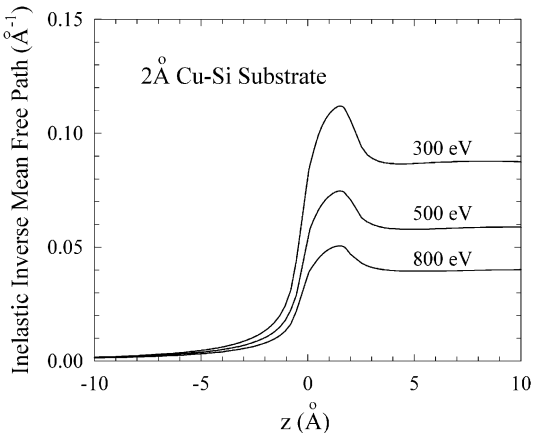

Fig. 4. The depth-dependent inelastic inverse mean free path for electrons of several energies normally incident on a vacuum-Cu–Si overlayer system with a 2 Å Cu film. Results were calculated using the extended Drude-type dielectric function [13] derived from experimental optical data [18].

system approaches that for semi-infinite Si. On the other hand, the electron inelastic inverse mean free path in the overlayer system for increasing film thickness approaches that for semi-infinite Cu. In Fig. 4, we plot the inelastic inverse mean free paths for normally incident electrons of several energies on the vacuum-Cu–Si overlayer system with a 2 Å Cu film. This figure shows that the electron inelastic inverse mean free path decreases with increase of electron energy, as expected.

Fig. 5 shows MC results of the elastically reflected intensity for 300 eV electrons backscattered from the vacuum-Cu–Si overlayer system with different Cu film thicknesses. For comparison, corresponding results for electrons backscattered from semi-infinite Cu and semi-infinite Si systems are included. For thicker Cu films of the overlayer system, the angular distribution approaches results for the semi-infinite Cu system. The elastic reflection intensity at smaller escape angles is more pronounced and enhanced as the thickness of Cu film increases. This is understood by examining Figs. 1 and 2 in that elastic differential cross-sections at large scattering angles, corresponding to small escape angles for the single-scattering events, are greater in Cu than in Si. A comparison of curves A and D in Fig. 5 with the corresponding

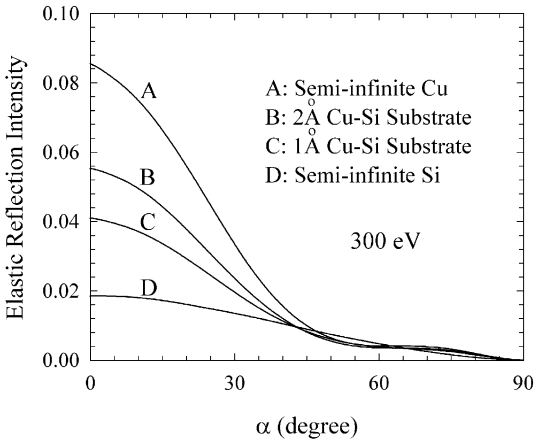

Fig. 5. MC results for the elastically reflected intensity for 300 eV normally incident electrons backscattered from the vacuum-Cu–Si overlayer system with different Cu film thicknesses as a function of emission angle.

curves in Figs. 1 and 2 reveals the importance of single-scattering events to the elastically reflected intensity. In Fig. 6, we plot the elastic reflection intensity for normally incident electrons of several energies on the vacuum-Cu–Si overlayer system with a 2 Å Cu film. It is seen that the intensity drops as the electron energy increases.

Fig. 7 shows MC results for the angular distribution of the elastically reflected intensity for 300 eV electrons backscattered from the vacuum-Cu–Si overlayer system with a 1 Å Cu film. The total and individual contributions from one to three elastic scatterings are shown. Here the single-scattering events contribute significantly to the elastically reflected intensity at small escape angles but less importantly at around 60°. The percentage contribution for all escape angles is 55.8% for single scattering, 22.3% for two scatterings, and 21.9% for a higher number of scatterings. To illustrate the contribution from single and multiple scatterings, we plot in Fig. 8 the percentage contributions from the indicated cumulative number of elastic scatterings to the elastic reflection intensity. This figure indicates that single-scattering events contribute more than half of the elastic reflection intensity for emission angles smaller than 40° and greater than 75°. Multiple (more than 3) scattering events contribute their largest proportion of 20% to the elastically reflected intensity for emission angles of around 60°. For the case of the 2 Å Cu film, similar conclusions may be drawn as the 1 Å case. Fig. 9 is a comparison of the angular distributions of the elastically reflected intensity calculated using Eqs. (12)–(17) and MC simulations for the contribution from single-scattering events for 300 eV electrons backscattered from the vacuum-Cu–Si overlayer system with 1 and 2 Å Cu films. Excellent agreement is found for each Cu thickness. A plot of the normalized angular distribution using Eq. (22) with $a = 0.8$ for 300 eV electrons backscattered from the overlayer system

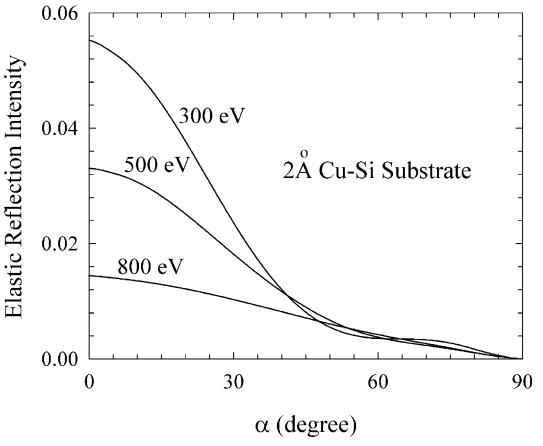

Fig. 6. MC results for the elastically reflected intensity for normally incident electrons of several energies backscattered from the vacuum-Cu–Si overlayer system with a 2 Å Cu film as a function of emission angle.

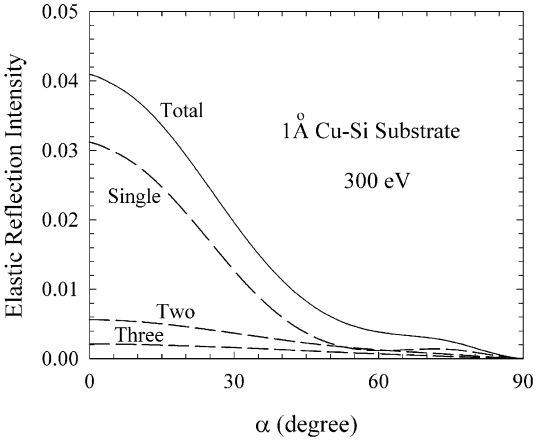

Fig. 7. A plot of the MC results for the elastically reflected intensity for 300 eV electrons backscattered from the vacuum-Cu–Si overlayer system with a 1 Å Cu film as a function of emission angle. Individual contributions from one, two and three elastic scatterings are shown separately.

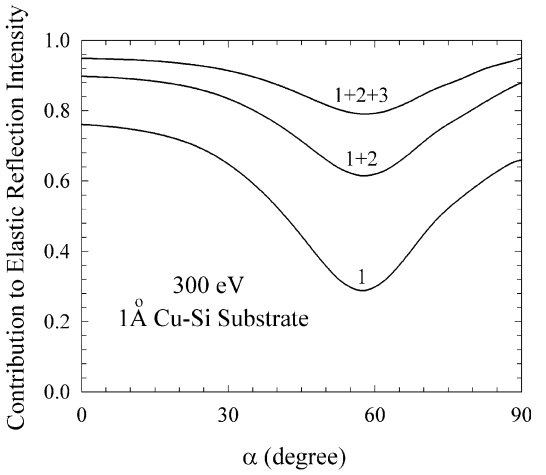

Fig. 8. MC results for the percentage contributions from one, two and three elastic scatterings to the elastically reflected intensity for 300 eV electrons elastically backscattered from the vacuum-Cu–Si overlayer system with a 1 Å Cu film as a function of emission angle.

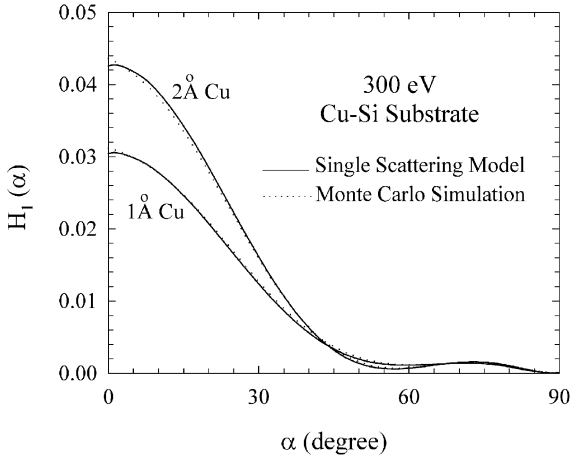

Fig. 9. A comparison of the elastically reflected intensity due to single-scattering events calculated using Eqs. (12)–(17) (—) and MC simulations (···) for 300 eV electrons backscattered from the vacuum-Cu–Si overlayer system with 1 and 2 Å Cu films.

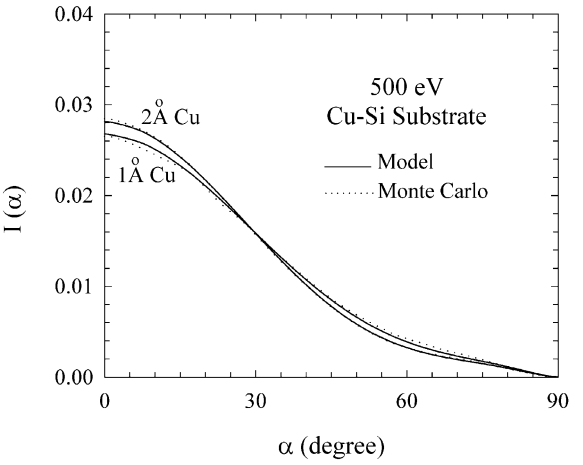

Fig. 11. A comparison of the normalized angular distribution of the elastically reflected intensity calculated using Eq. (22) with $a = 0$ (—) and MC simulations (···) for 500 eV electrons backscattered from the overlayer system with 1 and 2 Å Cu films.

with 1 and 2 Å Cu films is shown in Fig. 10. The corresponding MC results are included in this figure for comparison. Again, good agreement is found. Fig. 11 is a similar plot for 500 eV electrons. Since in this case the P_1-approximation is adequate to describe the angular distribution due to double scattering, we take $a = 0$. Note that the percentages of the individual contributions due to different numbers of elastic scatterings and the fitting parameter a in Eq. (22) are film-thickness independent; they are dependent only on electron energy. The percentage of contributions from single-scattering events is 66% for 500 eV electrons.

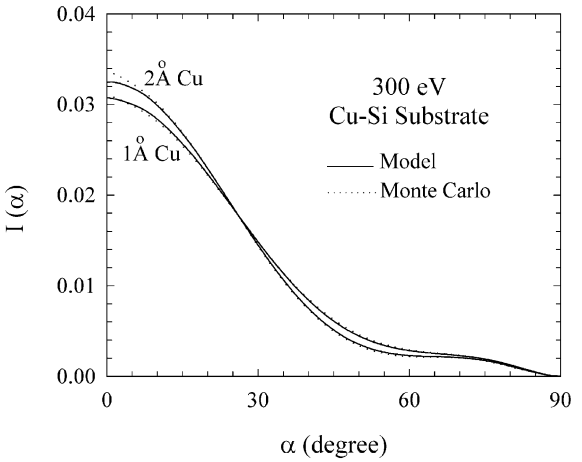

Fig. 10. A comparison of the normalized angular distribution of the elastically reflected intensity calculated using Eq. (22) with $a = 0.8$ (—) and MC simulations (···) for 300 eV electrons backscattered from the overlayer system with 1 and 2 Å Cu films.

5. Conclusions

We have derived formulations for the angular distribution of the elastically reflected intensity of electrons backscattered from vacuum-film–substrate overlayer systems. These formulations involved the evaluation of single-scattering events exactly, a combination of the single-scattering theory and the P_1-approximation for two elastic scatterings, and the P_1-approximation for multiple scatterings. All relevant inelastic interactions including volume excitations, surface (vacuum–film interface) excitations, and interface (film–substrate interface) excitations are considered. Comparison of the results calculated using these formulations and MC simulations for electrons elastically

backscattered from vacuum-Cu–Si overlayer systems shows close agreement.

The present approach is applicable to overlayer systems of amorphous and polycrystalline solids. For single crystals, crystalline diffraction focuses electrons in certain direction depending on the orientation. This effect is diminished in non-crystalline solids due to random elastic scattering [19,20].

Acknowledgements

This research was supported by the National Science Council of the Republic of China under contract no. NSC89-2215-E-009-048.

References

[1] J. Kirschner, P. Staib, Phys. Lett. 42 (1973) 335.
[2] J. Kirschner, P. Staib, Appl. Phys. 6 (1975) 99.
[3] G. Gergely, Surf. Interf. Anal. 3 (1981) 201.
[4] A. Jablonski, Surf. Sci. 151 (1985) 166.
[5] B. Gruzza, C. Pariset, Surf. Sci. 247 (1991) 408.
[6] C. Jardin, G. Gergely, B. Gruzza, Surf. Interf. Anal. 19 (1992) 5.
[7] W. Dolinski, S. Mröz, M. Zagórski, Surf. Sci. 200 (1988) 361.
[8] H. Beilschmidt, I.S. Tilinin, W.S.M. Werner, Surf. Interf. Anal. 22 (1994) 120.
[9] J.S. Schilling, M.B. Webb, Phys. Rev. B 2 (1970) 1665.
[10] A.L. Tofterup, Phys. Rev. B 32 (1985) 2808.
[11] Y.F. Chen, C.M. Kwei, P. Su, J. Phys. D: Appl. Phys. 28 (1995) 2163.
[12] A. Jablonski, H.S. Hansen, C. Jansson, S. Tougaard, Phys. Rev. B 45 (1992) 3694.
[13] C.M. Kwei, S.Y. Chiou, Y.C. Li, J. Appl. Phys. 85 (1999) 8247.
[14] Y.F. Chen, P. Su, C.M. Kwei, C.J. Tung, Phys. Rev. B 50 (1994) 17547.
[15] C.M. Kwei, P. Su, Y.F. Chen, C.J. Tung, J. Phys. D: Appl. Phys. 30 (1997) 13.
[16] C.M. Kwei, Y.F. Chen, C.J. Tung, J. Phys. D: Appl. Phys. 31 (1998) 36.
[17] C.M. Kwei, C.Y. Wang, C.J. Tung, Surf. Interf. Anal. 26 (1998) 682.
[18] C.M. Kwei, Y.F. Chen, C.J. Tung, J.P. Wang, Surf. Sci. 293 (1993) 202.
[19] S. Tougaard, I. Chorkendorff, Phys. Rev. B 35 (1987) 6570.
[20] R.F. Egerton, Electron Energy-loss Spectroscopy in the Electron Microscope, Plenum, New York, 1986.